Heliyon 9 (2023) e13206

Contents lists available at ScienceDirect

Heliyon

journal homepage: www.cell.com/heliyon

Research article

Analysis of riboflavin/ultraviolet a corneal cross-linking by molecular spectroscopy

Steven Melcher [a,*], Cordelia Zimmerer [b], Roberta Galli [a], Jonas Golde [a], Robert Herber [c], Frederik Raiskup [c], Edmund Koch [a], Gerald Steiner [a]

[a] Clinical Sensoring and Monitoring, Anesthesiology and Intensive Care Medicine, Technische Universität Dresden, Fetscherstrasse 74, 01307 Dresden, Germany
[b] Leibniz Institute of Polymer Research Dresden, Hohe Strasse 6, 01069 Dresden, Germany
[c] Department of Ophthalmology, University Hospital Carl Gustav Carus, Technische Universität Dresden, Fetscherstraße 74, 01307 Dresden, Germany

ARTICLE INFO

Keywords:
Collagen
Corneal cross-linking
Riboflavin
Keratoconus
Surface enhanced Raman spectroscopy

ABSTRACT

Corneal cross-linking (CXL) with riboflavin and ultraviolet A light is a therapeutic procedure to restore the mechanical stability of corneal tissue. The treatment method is applied to pathological tissue, such as keratoconus and induces the formation of new cross-links. At present, the molecular mechanisms of induced cross-linking are still not known exactly. In this study, we investigated molecular alterations within porcine cornea tissue after treatment with riboflavin and ultraviolet A light by surface enhanced Raman spectroscopy (SERS). For that purpose, after CXL treatment a thin silver layer was vapor-deposited onto cornea flaps. To explore molecular alterations induced by the photochemical process hierarchical cluster analysis (HCA) was used. The detailed analysis of SERS spectra reveals that there is no general change in collagen secondary structure while modifications on amino acid side chains are the most dominant outcome. The formation of secondary and aromatic amine groups as well as methylene and carbonyl groups were observed. Even though successful cross-linking could not be registered in all treated samples, Raman signals of newly formed chemical groups are already present in riboflavin only treated corneas.

1. Introduction

Keratoconus is a pathological condition where the central cornea is progressively thinned resulting in protrusion of the tissue. In many cases, keratoconus leads to astigmatism and worsening of visual acuity, which in severe cases can only be treated by corneal transplantation. Previous attempts to explain the loss of corneal integrity in keratoconus eyes have assumed changes in the orientation of the collagen fibrils [1], enzyme-mediated loss of collagen [2], increased oxidative damage [3,4] or failed fibrillogenesis [5].

Since cross-links of the collagenous matrix play a critical role in the maintenance of its optical and biomechanical properties, treatment approaches are aimed to generate new protein cross-links and to stabilize the tissue.

There are two major types of cross-links that naturally occur and stabilize the corneal tissue., The enzymatic cross-linking is the most abundant type [6]. It is based on oxidative deamination of the ϵ-amino group of lysine residues between collagen molecules

* Corresponding author.
E-mail address: steven.melcher@tu-dresden.de (S. Melcher).

https://doi.org/10.1016/j.heliyon.2023.e13206
Received 25 May 2022; Received in revised form 19 January 2023; Accepted 20 January 2023
Available online 24 January 2023

resulting in the formation of Schiff base type bonds. Another type is a non-enzymatic cross-linking (glycation). Reactions between glucose and free aldehyde groups lead to advanced glycation end-products (AGEs). Glycation is a major contributor to changes in biomechanics with age.

To enhance biomechanical properties of the corneal tissue and counteract worsening of keratoconus, photochemical cross-linking with riboflavin as photosensitizer and ultraviolet light irradiation has been developed [7]. The standard protocol involves removing the central 10 mm of the epithelium and treating the cornea with 0,1% riboflavin solution for 30 min. The cornea is then exposed to ultraviolet light (370 nm, 3 mW/cm^2) for 30 min [8]. There are clinically used modifications of the standard protocol that use higher intensity light up to 9 mW/cm^2 for 10 min (accelerated CXL) with application of the same energy dose resulting in similar stiffening of the cornea [9].

The CXL treatment is assumed to lead to photochemical polymerization and generation of new covalent bonds within collagen fibrils involving the formation of singlet oxygen and other reactive oxygen species (ROS), thus enhancing the biomechanical properties of the cornea [10,11]. Although several macroscopic effects like increased tissue stiffness [12,13], higher resistance to enzymatic digestion [14] or changes in fibril architecture [15] have been reported, only a limited number of studies has investigated CXL on a

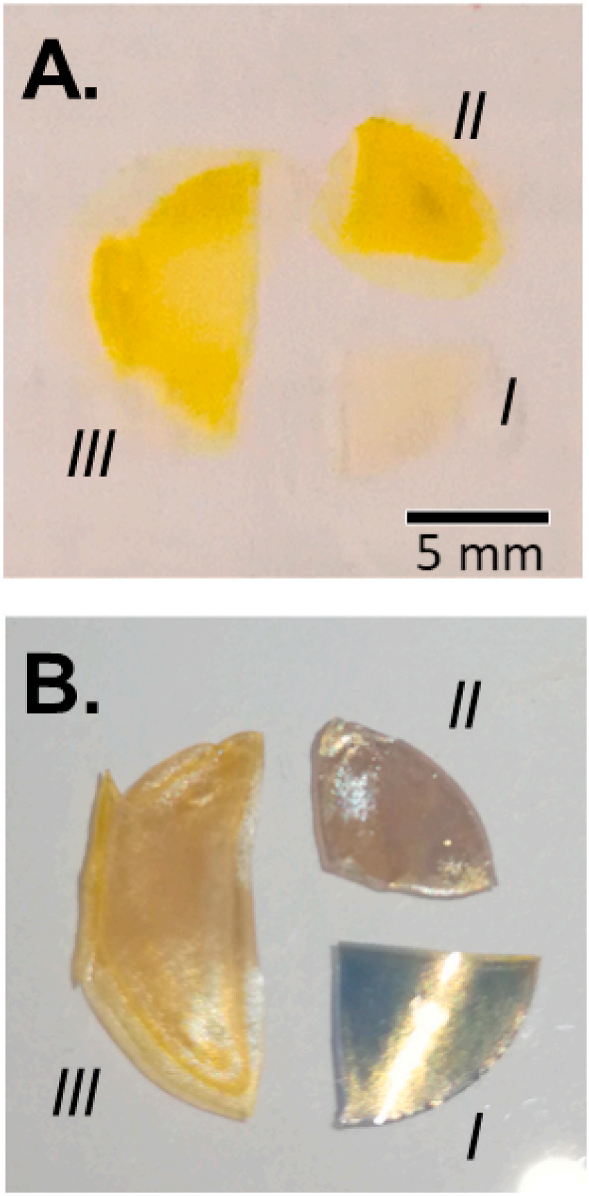

Fig. 1. Cornea Flaps of 160 μm thickness are divided into three segments as shown. This segmentation was chosen to make it easier to cut the flaps. (A) depicts the samples before and (B) after application of silver layer. Group I is the untreated control group. Group II has been treated with riboflavin only and group III has been treated with riboflavin and ultraviolet light.

molecular level [10,16–20]. Since the available literature offers various findings about the induced cross-links (e.g., ether type bonds, amide bonds, dityrosine cross-links), characterizing the biochemical changes of the cross-linking process might provide not only better understanding of the process itself but also provide valuable information to adapt clinical parameters (e.g., treatment time) towards an increased efficiency of the overall process and improvements of the patient outcome.

In recent years several methods, such as fluorescence spectroscopy [21], mass spectrometry [22,23] or gel electrophoresis [19], were published for the determination of cross-links in proteins. However, none of these methods directly target molecular mechanisms of cross-linking. Molecular spectroscopic techniques, such as Infrared and Raman spectroscopy are non-destructive approaches for structural analysis of many disease related molecular mechanisms. In particular, Surface Enhanced Raman Spectroscopy (SERS), a special type of Raman spectroscopy, provides highly specific molecular information and offers a superior sensitivity [24].

The presented work aims to investigate the molecular alterations induced by CXL treatment. Since Raman spectroscopy is a technique that can asses collagen bond formation it can be used to better describe the nature of the crosslinks and limit the number of possible mechanisms leading to its creation. For this purpose, we used porcine cornea as a model for human cornea. The identification of molecular alterations induced by riboflavin and ultraviolet A light was performed by using SERS in combination with a multivariate data analysis. Understanding the molecular processes of cornea cross-linking will drive knowledge on the molecular mechanisms of CXL treatment and is therefore also an essential presumption for an individual and optimized therapy.

2. Material and methods

2.1. Sample preparation and cross-linking procedure

Fresh pig eyes were received from a local slaughterhouse. The eyes are a waste product and no pig was sacrificed specifically for this study. The fresh eyes were transported refrigerated and used for sample preparation within 6 h on the day of delivery. After extra-ocular tissue had been removed all eye globes were de-epithelialized using a scalpel. Central corneal flaps 160 μm thick were cut with a lamellar rotating microkeratome (Amadeus I, Ziemer Ophthalmic Systems, Port, Switzerland). Corneal flaps have to be used since silver deposition under high vacuum conditions would not have been possible for an intact eye. Subsequently each sample flap was divided into 3 segments as shown in Fig. 1A. One segment was used as control sample (group I), the second segment sample was treated with riboflavin but not irradiated with UV light (group II) and finally the third segment sample was treated with riboflavin and ultraviolet light (group III). Samples of group II and III were soaked in 0.1% riboflavin solution with 10% dextran for 10 min. Immediately after soaking, samples of group III were irradiated with ultraviolet light (370 nm, 9 mW/cm^2) for 10 min according to the accelerated CXL protocol [9]. During irradiation, small drops of Riboflavin solution were applied two times within the 10 min to prevent the tissue from drying. The accelerated CXL protocol used here shows similar effectiveness in stiffening the cornea compared to the standard protocol but is much less likely to be affected by dehydration effects of the upper corneal layers [25,26]. In contrast to the standard protocol, a 10% dextran solution was used to avoid further possible dehydration. A loss of water in the cornea would also lead to distinct signals in the Raman spectra and thus overlay the molecular signals of the induced stiffening. The accelerated protocol induces stiffening preferentially in the upper layers of the cornea. In the examinations of the prepared corneal samples, stiffening of the deeper layers can be omitted, since the high mechanical strength as in the actual therapeutic application does not have to be achieved here and SERS is a surface analytical method. Finally, all samples were placed on object slides and sent for further sample preparation.

2.2. Polarization-sensitive OCT imaging

Prior to deposition of the silver layer and Raman spectroscopy, cross-linking in the upper third of the stromal tissue was verified by polarization-sensitive optical coherence tomography (PSOCT) perfomed with the PSOCT system (TEL220PSC2, Thorlabs GmbH, Germany) with a spectral range around 1300 nm was applied for imaging porcine eyes before and after ultraviolet illumination. Similar to the described sample preparation, intact eyes instead of flaps were accordingly treated and cross-linked by riboflavin and ultraviolet illumination. Acquired cross-sectional images were processed by a custom Matlab (MathWorks Inc., Natick, USA) software

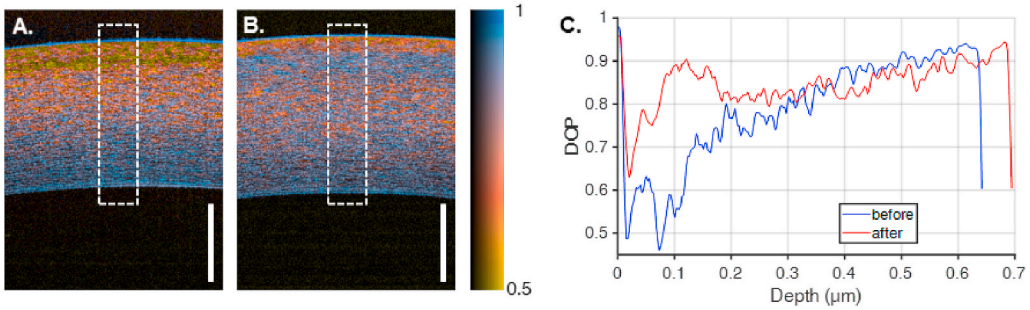

Fig. 2. Representative cross-sectional depolarization images of porcine cornea before ultraviolet illumination (A) and after ultraviolet illumination (B) in CXL treatment process. Scale bars correspond to 300 μm. (C) Depth-resolved, i.e. anterior to posterior direction, plot of mean DOP values for marked ROIs.

routine and the degree of polarization (DOP) was calculated [27]. A refractive index of 1.38 [28] was assumed for specifying depth information.

Previous studies indicate that the effective cross-linking region is not homogenous throughout the corneal stroma but mostly located in the upper third [29]. Since corneal tissue consists of highly organized collagen fibrils it exhibits both birefringent and depolarizing properties. Changes of the polarization-related properties can be analyzed by use of PSOCT. To verify the effective cross-linking depth of prepared samples PSOCT cross-sectional images before ultraviolet illumination (A) and after ultraviolet illumination (B) are registrated shown in Fig. 2., The different depolarization contrasts between Fig. 2A and B indicate that the cross-linking treatment induces a change in the optical properties of the birefringent corneal stroma. As visualized in the related depth-resolved plots (C), this effect is most pronounced in the uppermost 200 μm of the stroma. Although the limited axial resolution and a strong corneal surface reflex limit insights on changes in the first molecular layer, the treatment results in a less pronounced depolarizing anterior stroma which we assume includes the corneal surface. We hypothesize that these conditions can be explained by changed patterns of collagen fibril organization. It is important to note that the variable size and shape of nanoparticles in the silver layer for SERS experiments make it impossible to determine a precise penetration depth of the plasmon field into the cornea tissue structure. However, surface topography and roughness of the dried cornea might benefit the formation of Ag nanoparticles aggregates. Thus, we assume that the penetration depth of the plasmon field is much larger than few nanometers, as it would be for ideal and isolated nanoparticles. Since significant molecular alterations are localized in the anterior stroma, SERS spectra of cross-linked corneal tissue have been obtained for the first time by enhancing signal intensities in corneal tissue that is in contact with the silver layer (Fig. 3).

2.3. Preparation of silver layer

Before applying the silver layer, corneal tissue was tempered for 24 hand pre-dried under vacuum for 73 h at 37 °C and a pressure of $4{\cdot}10^{-4}$ bar. The samples silver layer was deposited in the vacuum chamber (Creamet 300 V2, Creavac, Germany) at a constant rate of 0.01 nm/s for 8 min resulting in a layer thickness of roughly 5 nm. Fig. 1B shows the resulting samples after deposition of the silver layer.

2.4. Raman spectroscopy

Raman spectra were recorded in reflection configuration using a RamanRXn spectrometer (Kaiser Optical Systems Inc., Ann Arbor, USA) coupled to a light microscope (DM2500 P, Leica Microsystems GmbH, Wetzlar, Germany). Raman signals were excited by a 785 nm diode laser (Invictus 785 nm NIR, Kaiser Optical Systems Inc., Ann Arbor, USA). The light was focused on the sample surface with an Olympus objective (20×/NA = 0.45) resulting in a spot size of around 50 μm. The laser power was set to 200 mW. For each cornea sample five Raman spectra from different points were acquired by averaging 20 individual spectra with an exposure time of 2 s each. The spectral range was 400 cm^{-1} – 3250 cm^{-1} and the spectral resolution was 4 cm^{-1}. Table 1 summarizes the recorded spectra for each sample group.

2.5. Spectral data processing

Spectroscopic data pre-processing and hierarchical cluster analysis was performed using Matlab (MathWorks Inc., Natick, USA). First, all spectra were reduced to the spectral range of 500 cm^{-1}-1800 cm^{-1}. In order to minimizes noise scattering, Savitsky-Golay smoothing was applied (11-point window size and third-degree polynomial). Spectra were corrected by subtracting a linear

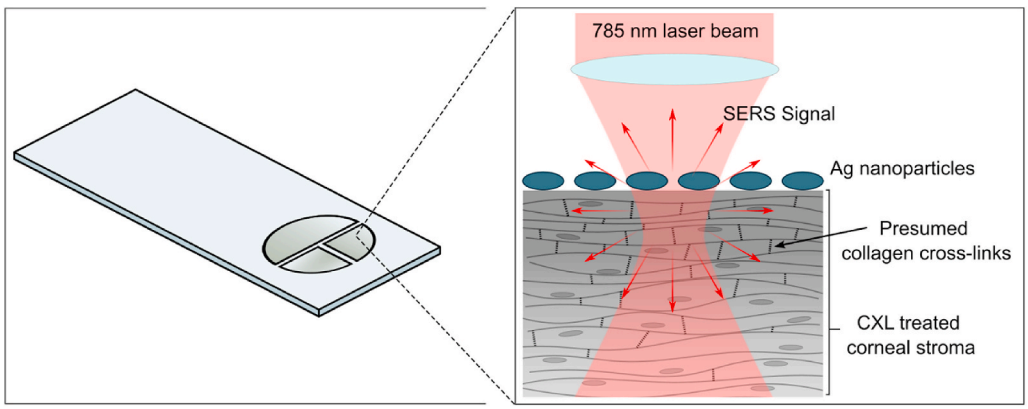

Fig. 3. Schematic drawing of the experimental setup for SERS of porcine cornea flaps. Samples are placed on calcium fluoride slides to minimize the background signal. The exciting laser beam is focused on the surface where cross-links are believed to have the highest density and backscattered light is collected through the objective for spectral analysis.

Table 1
Spectra collected for each group and number of samples.

Group	Treatment	Number of samples	Spectra obtained
I	Control	10	50
II	Riboflavin only	10	50
III	Riboflavin and ultraviolet light	10	50

baseline fitted on manually defined points ($\overline{\nu_1}$, $\overline{\nu_1}$ +5 cm^{-1}, 630 cm^{-1}, 1140 cm^{-1}, 1505 cm^{-1}, $\overline{\nu}_2$-10 cm^{-1}, $\overline{\nu}_2$-5 cm^{-1} and $\overline{\nu}_2$ where $\overline{\nu_1}$ and $\overline{\nu}_2$ 500 cm^{-1} and 1800 cm^{-1}, respectively) followed by vector normalization. Hierarchical clustering dendrograms were calculated with City Block distance metric and average distance clustering.

3. Results and discussion

3.1. Raman spectra of the cornea samples

To access molecular alterations induced by the CXL treatment, individual spectra were collected on non-treated samples (group I), on riboflavin only treated samples (group II) and riboflavin and ultraviolet treated samples (group III). Fig. 4A displays the calculated mean spectrum and bands of standard deviation of raw spectra for each of the three groups in the spectral range of 400–3200 cm^{-1}. Spectra of group III show the highest SERS intensities but also strong variations. Spectra of group II and group III show a fluorescence background in addition to the collagen signals, which cannot be observed in group I. The fluorescence background is more pronounced in spectra of group III compared to spectra of group II. We assume that fluorescence is induced by molecular alterations after CXL treatment. Even though samples of group II and III are treated with riboflavin in the same way, no absorption bands of riboflavin (Appendix Fig. 1) can be found in the recorded spectra. Fig. 4B displays the calculated mean SERS spectra after smoothing, baseline correction and vector normalization in the spectral region between 400 and 1800 cm^{-1}. Main spectral features are the amid I and amid III band centered around 1650 cm^{-1} and 1250 cm^{-1}, respectively. The signal at 1450 cm^{-1} is assigned to CH_x-deformation modes. The region between 850 and 950 cm^{-1} is composed of different C–C protein backbone modes as well as C–C vibrations of proline amino acids. All three groups show a nearly identical intensity of the phenylalanine band at 1001 cm^{-1} which is an important marker for the protein content. Table 2 lists the main spectral features and band assignments of the SERS spectra of cornea [30,31,32,33]. Closer

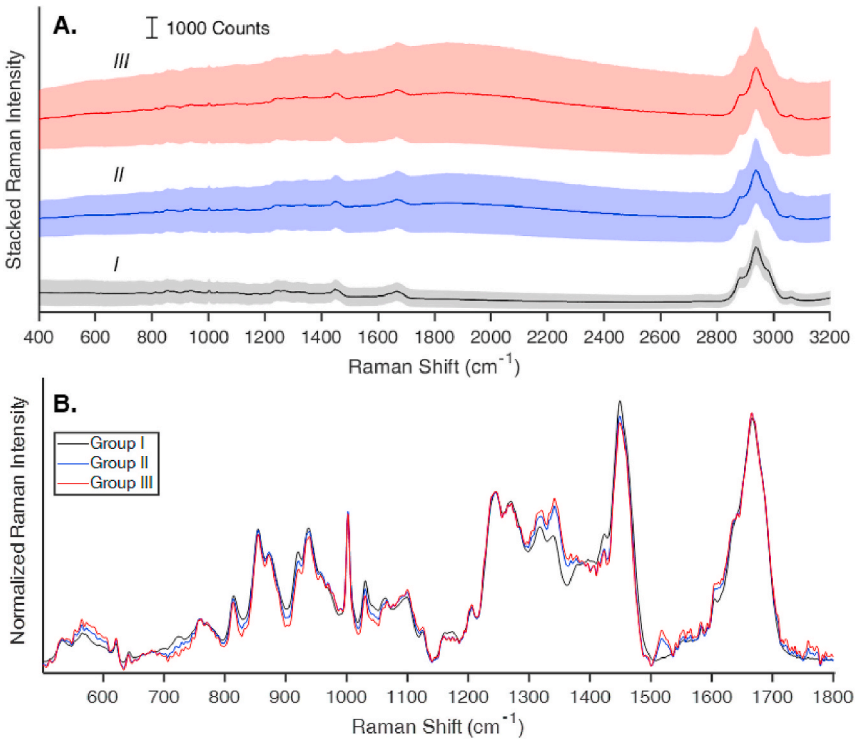

Fig. 4. (A) Mean and standard deviation of the raw Raman spectra cornea flaps from 10 different porcine eyes. Control group I black (n=50), Riboflavin only group II blue (n=50), Riboflavin and ultraviolet treated group III red (n=50). (B) Mean Raman spectra after correction for baseline and fluorescence, smoothing and normalization in the spectral region 500-1800 cm^{-1}. (For interpretation of the references to color in this figure legend, the reader is referred to the Web version of this article.)

inspection of the spectral data shows a very similar behavior for the two treated sample groups II and III, however differences between these are way more subtle and need to be analyzed in detail. Therefore, the spectral data was subjected to a hierarchical cluster analysis.

3.2. Cluster analysis

Fig. 5 shows the results of hierarchical cluster analysis. The dendrogram displays two distinct main branches with different numbers of sub clusters. While cluster ① contains with 94 spectra (63% of all spectra) by far the majority of the entire data set, seven clusters (②,③,④,⑤,⑦,⑨,⑩) of the other main branch represent together only 20 spectra (13%) predominantly belonging to group III. Another larger cluster (⑥) contains 35 spectra (23%) of group II and group III. The dendrogram indicates no clear separation between spectra of the three groups. Moreover, the branching pattern shows further inconsistencies in the data set. Spectra of group I are represented only by cluster ①. It should be noted that the immediately neighboring cluster ⑧ contains only one spectrum of group I. Spectra of group II are nearly equally distributed between clusters ① and ⑥. 18 spectra of group III are unequally distributed on seven clusters. The most surprising result is that 32 spectra of group III are assigned to cluster ① and ⑥, respectively. Furthermore, the 18 spectra of the other main branch represent only 6 samples. Overall, the results of hierarchical cluster analysis point to a scenario where the expected cross-linking process accompanied by molecular alterations cannot be observed in all recorded SERS spectra and is, in general, not apparent in all treated samples. Fig. 6 shows the spectra grouped to three classes according to their cluster assignment and group membership. Only 26 out of 50 spectra of the fully treated samples could be assigned to either class 2 (“transition state”) or class 3 (“cross-linked state”), therefore the cross-linking effect is only observable in around 50% of the spectra. To date, several studies have investigated the stiffening effect of cross-linking treatment with different methods (c.f., [34,35,36]) and it could conceivably be hypothesized that the CXL treatment does not cause substantial molecular alterations in each individual cornea. This leads to high variations between individual samples and difficulties in distinguishing them [37]. Furthermore, clinical benefits of CXL can differ among patients where several cases show a continued progression of corneal ectasia [38,39]. However, the observation of spectral differences distinguishing spectra of group III from group I and II indicates that molecular alterations must be present after the cross-linking procedure at least in a subset of samples. Thus, the question arises which molecular alterations can be identified.

Although the spectral profiles in Fig. 6A appear to be quite similar at first glance, a closer inspection of the calculated mean spectra, shown in Fig. 6B, reveals five regions of the spectrum that stand out clearly as characteristic for each of the three classes. The most prominent features are the spectral profiles centered at 1518 cm^{-1} and between 1304 cm^{-1} to 1365 cm^{-1}, which increase progressively from class 1 to 3. Also, the weaker signals between 1080 cm^{-1} and 1132 cm^{-1}, at 1604 cm^{-1} and between 1750 cm^{-1} to 1772 cm^{-1} show a similar behavior. Among all distinct features, only the band at 1517 cm^{-1} is not present in spectra of class 1. This band can be assigned to secondary or aromatic amines which have a Raman active C–N–H bending mode around 1510 cm-1 [33]. This is underlined by the signal at 1604 cm^{-1} that also represents a C–N–H scissoring band. It should be noted that possible interferences in this region are from the aromatic ring or hetero ring modes. The signals between 1304 cm^{-1} and 1365 cm^{-1} are assigned to deformation modes of CH_2 groups (c.f. Table 2). The pattern of bands between 1080 cm^{-1} and 1132 cm^{-1} can be assigned to C–N and C–C–C modes. The signal between 1750 cm^{-1} and 1772 cm^{-1} is attributed to the C═O vibration which is generally weak in Raman spectra. As already mentioned above, all these signals increase from class 1 to 3. Only the signal at 1450 cm^{-1} exhibits a slight opposite trend. The spectral profile of collagen is in all three classes present and no significant band shift could be observed, which suggests no general changes in the collagen secondary structure. Thus, the hypothesis based on these findings is that amino acid side chains of the collagen backbone are predominantly involved in the initiated cross-linking process. The results are in line with those of previous studies that consider bonds between amino acid side chains as the most dominant result of CXL [10,16,18]. Jung et al. investigated the effects of CXL treatment on the human sclera with Raman spectroscopy [16]. In this study, the tissue was cross-linked according to the Dresden protocol. Spectroscopic data revealed a simultaneous shift of the C–C–C (around 393 cm^{-1}) and S–S (401 cm^{-1}) strech band to higher wavenumbers. A new band appeared at 1126 cm^{-1} (C–N) and at the same time the intensity of the CH_2 mode located between 1322 cm^{-1} and 1338 cm^{-1} is increased. These changes of C–N and CH_2 bands were also evident in the spectra of the cornea. It seems

Table 2
Main Raman bands and their assignments in cornea samples (ν = stretching vibration, δ = deformation vibration, γ_w = wagging out of plane, γ_t = twisting out of plane).

Raman Shift (cm^{-1})	Assignment
814–922	ν(C–C) of proline/hydroxyproline
938	ν(C–C) of protein backbone
1003	phenylalanine
1099	ν(C–N)
1245	Amide III, δ(NH)
1271	Amide III, δ(NH)
1318	γ_t (CH_2)
1341	γ_w (CH_2)
1450	$\delta(CH_2)/\delta(CH_3)$
1517	δ(CNH) of aromatic/secondary amines
1666	Amid I, ν(C═O)

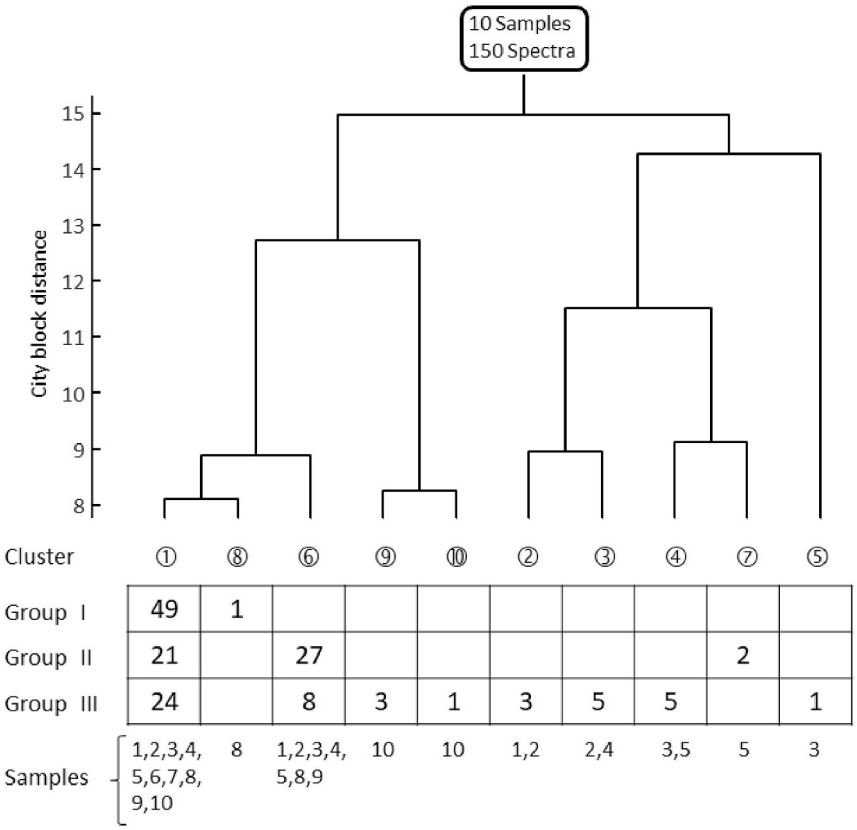

Fig. 5. Dendrogram of the hierarchical cluster analysis. The table indicates the membership of SERS spectra, belonging to group I, II or III and the assignment of spectra to individual samples.

plausible that molecular alterations in scleral tissue are of the same origin as in corneal tissue.

The fact that modes of amino groups appear as well as the increased intensities of bands associated with CH_2 groups clearly points to molecular processes associated with the formation of secondary or aromatic amino groups and methylene groups. This is also supported by the growing intensities of C–N modes. The minimal decrease of the band centered at 1450 cm^{-1} indicates a degradation of chemical groups causing C–H deformation modes in this region.

Since many spectra of class II show features similar to class III, we suppose the existence of a transition state where the number of cross-links increases. This transition state contains signals that are also characteristic for class III (1518 cm^{-1}, between 1304 cm^{-1} and 1365 cm^{-1}, 1080 - 1132 cm^{-1}, 1604 cm^{-1} and 1750 - 1772 cm^{-1}) but less pronounced. The 29 samples of class II belong to group II that are samples treated with riboflavin only. We assume that samples are already altered partially by ultraviolet radiation of the ambient light, which leads to the production of sufficient ROS to start the cross-linking process [7]. This would be plausible since contact of the sample with ambient light was not blocked during the incubation time in riboflavin. It should be mentioned that quantification of the spectral signals, especially the changes, is helpful for the interpretation of the molecular processes. However, since a reliable referencing is required for this purpose and corresponding standards for the molecular processes of corneal stiffening are not yet known, no quantification of the spectral signals can be performed.

The detailed evaluation of the spectra leads to the conclusion that molecular bonds alone do not cause the changed mechanical properties. While the spectroscopic data show the formation of bonds, these alone do not explain the macroscopic picture. The presented results show that molecular bonds are involved in the crosslinking but it cannot be concluded that covalent bonds occur between individual collagen chains. We assume that due to the ROS initiated processes weak molecular bonds like polar-polar or hydrophobic-hydrophobic interaction between collagen chains become more pronounced, leading to an enhanced mechanical stability of corneal tissue. However, an inherent limitation of the technique lies in the registration of weak molecular bonds that cannot be detected directly by Raman or SERS, if at all. Although the formation of side groups, especially amino and carbonyl groups with a high polar fraction, also lead to weak polar interactions, these forces cannot be detected by the spectroscopic methods. Furthermore, it must be considered that the molecular matrix, i.e. the collagen backbone, remains unchanged in its secondary structure and that comparatively few molecular changes account for stiffening. The results of the study refute the hypothesis that covalent bonds between side groups of the collagen chains are primarily the cause of mechanical stiffening after CXL treatment.

From clinical view, the CXL procedure is an established treatment that stabilized a progressive keratoconic cornea over years [40, 41,42], where the failure rate is very low for the standard protocol (7.5%) as well as accelerated protocols (13.6%) [43]. This is in

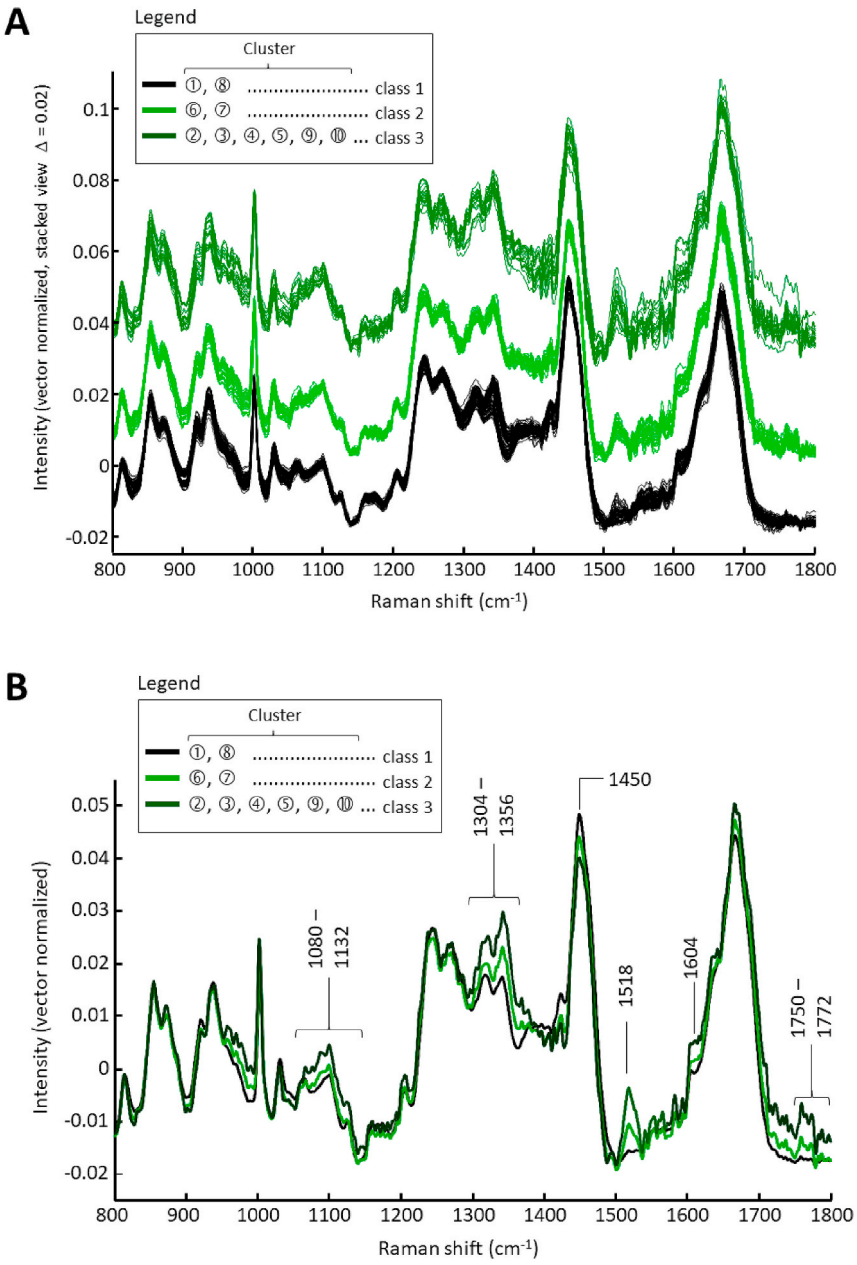

Fig. 6. (A) Plot of spectra summarized to three classes and colored according to their cluster membership as indicated in the legend. (B) calculated mean spectra of the three classes.

contrast to the observed cross-linking effect in the presented study were only 50% of the treated samples have shown molecular alterations. This also points to the theory that increased cornea stiffness is created not only by new molecular bonds but also by other processes which are not associated with structural changes. Based on other ex vivo investigations, CXL increases the corneal tissue measureable by a higher Young's modulus [12]. This was also evident using other methods such as inflation tests [44] or air-puff tonometry [45]. Furthermore, a biomechanical stiffening effect was also found In vivo [46]. In general, deviations from successful CLX treatment of keratoconus show that in addition to a molecular crosslinking, further changes in the cornea also may lead to stiffening. However, these changes have not yet been extensively investigated. We conclude that formation of new molecular bonds of CLX treated corneas is one among other possible processes for an increased stiffness of the tissue.

4. Conclusion

Understanding the nature of the crosslinks formed by CXL is clinically relevant for improving the Dresden protocol or developing

new treatments for keratoconus. The study used SERS as a surface sensitive spectroscopic method to detect molecular changes, i.e. in particular the formation of new covalent bonds, in porcine corneal tissue treated with CXL. In about 50% of the samples examined, an increase in SERS bands assigned to amino groups was observed after CXL treatment. Similarly, stronger Raman signals from methyl and carbonyl groups were registered, which could contribute to further intermolecular forces and thus to corneal tissue stiffening. Changes in the secondary structure of collagen were not observed. The study thus refutes hypotheses that covalent bonds between protein side groups are a major cause of corneal stiffening after CXL treatment.

Author contribution statement

Steven Melcher, Gerald Steiner, Jonas Golde: Conceived and designed the experiments; Performed the experiments; Analyzed and interpreted the data; Wrote the Paper.

Cordelia Zimmerer: Conceived and designed the experiments; Analyzed and interpreted the data; Contributed reagents, materials, analysis tools or data.

Roberta Galli, Robert Herber, Frederik Raiskup, Edmund Koch: Conceived and designed the experiments; Analyzed and interpreted the data.

Funding statement

The author Steven Melcher was supported by the European Union/ESF and the Free State of Saxony within a doctoral scholarship (Project No. 100316833). The Article Processing Charges (APC) were funded by the joint publication fund of the TU Dresden, the Medical Faculty Carl Gustav Carus, and the SLUB Dresden.

Data availability statement

Data included in article/supp. material/referenced in article.

Declaration of interest's statement

The authors declare no competing interests.

Additional information

No additional information is available for this paper.

Acknowledgments

The authors would like to thank Toni Utech and Felix Schütze from the Leibniz Institute of Polymer Research Dresden for the preparation of silver layer. Furthermore, we thank the European Union/European Social Fund (ESF) and the Free State of Saxony for supporting this project.

Appendix

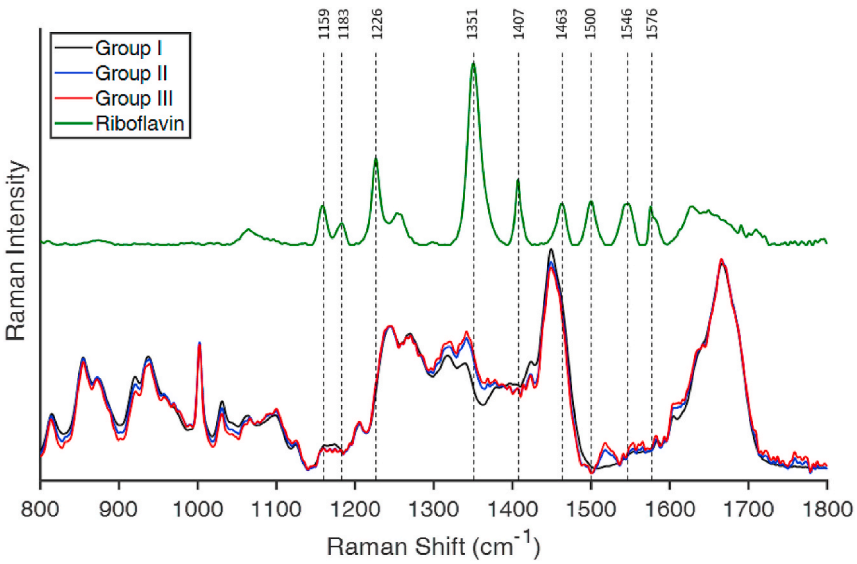

Fig. 1. Raman spectrum of Riboflavin and its major peaks (top) Mean Raman spectra of cornea flaps (bottom).

References

[1] P. Fratzl, Collagen fibril diameter in the human corneal stroma, Invest. Ophthalmol. Vis. Sci. 38 (1997) 121–129.
[2] T. Fukuchi, B.Y. Yue, J. Sugar, S. Lam, Lysosomal enzyme activities in conjunctival tissues of patients with keratoconus, Arch. Ophthalmol. 112 (1994) 1368–1374. http://www.ncbi.nlm.nih.gov/pubmed/7945042.
[3] T.D. Gondhowiardjo, N.J. van Haeringen, H.J. Volker-Dieben, H.W. Beekhuis, J.H.C. Kok, G. van Rij, L. Pels, A. Kijlstra, Analysis of corneal aldehyde dehydrogenase patterns in pathologic corneas, Cornea 12 (1993) 146–154, https://doi.org/10.1097/00003226-199303000-00010.
[4] A. Behndig, B. Svensson, S.L. Marklund, K. Karlsson, Superoxide dismutase isoenzymes in the human eye, Invest. Ophthalmol. Vis. Sci. 39 (1998) 471–475. http://www.iovs.org/content/39/3/471.short%5Cnhttp://www.ncbi.nlm.nih.gov/pubmed/9501855.
[5] S. Wilson, W. Kim, Keratocyte apoptosis: implications on corneal wound healing, tissue organization, and disease, Invest. Ophthalmol. Vis. Sci. 39 (1998) 220–226. http://citeseerx.ist.psu.edu/viewdoc/download?doi=10.1.1.320.7451&rep=rep1&type=pdf.
[6] M. Yamauchi, G.S. Chandler, H. Tanzawa, E.P. Katz, Cross-linking and the molecular packing of corneal collagen, Biochem. Biophys. Res. Commun. 219 (1996) 311–315, https://doi.org/10.1006/BBRC.1996.0229.
[7] E. Spörl, M. Huhle, T. Seiler, Induction of cross-links in corneal tissue, Exp. Eye Res. 66 (1998) 97–103, https://doi.org/10.1006/exer.1997.0410.
[8] G. Wollensak, E. Spörl, T. Seiler, Riboflavin/Ultraviolet-A-induced collagen crosslinking for the treatment of keratoconus, Am. J. Ophthalmol. 135 (2003) 620–627, https://doi.org/10.1016/S0002-9394(02)02220-1.
[9] J. Wernli, S. Schumacher, E. Spoerl, M. Mrochen, The efficacy of corneal cross-linking shows a sudden decrease with very high intensity UV light and short treatment time, Invest. Ophthalmol. Vis. Sci. 54 (2013) 1176–1180, https://doi.org/10.1167/iovs.12-11409.
[10] A.S. McCall, S. Kraft, H.F. Edelhauser, G.W. Kidder, R.R. Lundquist, H.E. Bradshaw, Z. Dedeic, M.J.C. Dionne, E.M. Clement, G.W. Conrad, Mechanisms of corneal tissue cross-linking in response to treatment with topical riboflavin and long-wavelength ultraviolet radiation (UVA), Investig. Opthalmol. Visual Sci. 51 (2010) 129–138, https://doi.org/10.1167/iovs.09-3738.
[11] S. Hayes, C.S. Kamma-Lorger, C. Boote, R.D. Young, A.J. Quantock, A. Rost, Y. Khatib, J. Harris, N. Yagi, N. Terrill, K.M. Meek, The effect of riboflavin/UVA collagen cross-linking therapy on the structure and hydrodynamic behaviour of the ungulate and rabbit corneal stroma, PLoS One 8 (2013), e52860, https://doi.org/10.1371/journal.pone.0052860.
[12] G. Wollensak, E. Spörl, T. Seiler, Stress-strain measurements of human and porcine corneas after riboflavin–ultraviolet-A-induced cross-linking, J. Cataract Refract. Surg. 29 (2003) 1780–1785, https://doi.org/10.1016/S0886-3350(03)00407-3.
[13] A. Hammer, O. Richoz, S.A. Mosquera, D. Tabibian, F. Hoogewoud, F. Hafezi, Corneal biomechanical properties at different corneal cross-linking (CXL) irradiances, Invest. Ophthalmol. Vis. Sci. 55 (2014) 2881–2884, https://doi.org/10.1167/iovs.13-13748.
[14] E. Spörl, G. Wollensak, T. Seiler, E. Spoerl, G. Wollensak, T. Seiler, E. Spörl, G. Wollensak, T. Seiler, Increased resistance of crosslinked cornea against enzymatic digestion, Curr. Eye Res. 29 (2004) 35–40, https://doi.org/10.1080/02713680490513182.
[15] G. Wollensak, M. Wilsch, E. Spoerl, T. Seiler, Collagen fiber diameter in the rabbit cornea after collagen crosslinking by riboflavin/UVA, Cornea 23 (2004) 503–507, https://doi.org/10.1097/01.ico.0000105827.85025.7f.
[16] G.-B. Jung, H. Lee, J. Kim, J.I. Lim, S. Choi, K.-H. Jin, H.-K. Park, I. Lim, S. Choi, Effect of cross-linking with riboflavin and ultraviolet A on the chemical bonds and ultrastructure of human sclera, J. Biomed. Opt. 16 (2011), 125004, https://doi.org/10.1117/1.3662458.
[17] P. Kamaev, M.D. Friedman, E. Sherr, D. Muller, Photochemical kinetics of corneal cross-linking with riboflavin, Invest. Ophthalmol. Vis. Sci. 53 (2012) 2360–2367, https://doi.org/10.1167/iovs.11-9385.
[18] S.-H. Chang, A. Mohammadvali, K.-J. Chen, Y.-R. Ji, T.-H. Young, T.-J. Wang, C.E. Willoughby, K.J. Hamill, A. Elsheikh, The relationship between mechanical properties, ultrastructural changes, and intrafibrillar bond formation in corneal UVA/riboflavin cross-linking treatment for keratoconus, J. Refract. Surg. 34 (2018) 264–272, https://doi.org/10.3928/1081597X-20180220-01.
[19] Y. Zhang, A.H. Conrad, G.W. Conrad, Effects of ultraviolet-A and riboflavin on the interaction of collagen and proteoglycans during corneal cross-linking, J. Biol. Chem. 286 (2011) 13011–13022, https://doi.org/10.1074/jbc.M110.169813.
[20] Y. Kato, K. Uchida, S. Kawakishi, Aggregation of collagen exposed to uva in the presence of riboflavin: a plausible role of tyrosine modification, Photochem. Photobiol. 59 (1994) 343–349, https://doi.org/10.1111/j.1751-1097.1994.tb05045.x.

[21] M.B. Applegate, B.P. Partlow, J. Coburn, B. Marelli, C. Pirie, R. Pineda, D.L. Kaplan, F.G. Omenetto, Photocrosslinking of silk fibroin using riboflavin for ocular prostheses, Adv. Mater. 28 (2016) 2417–2420, https://doi.org/10.1002/adma.201504527.
[22] M. Terajima, I. Perdivara, M. Sricholpech, Y. Deguchi, N. Pleshko, K.B. Tomer, M. Yamauchi, Glycosylation and cross-linking in bone type I collagen, J. Biol. Chem. 289 (2014) 22636–22647, https://doi.org/10.1074/jbc.M113.528513.
[23] A. Takaoka, N. Babar, J. Hogan, M. Kim, M.O. Price, F.W. Price, S.L. Trokel, D.C. Paik, An evaluation of lysyl oxidase–derived cross-linking in keratoconus by liquid chromatography/mass spectrometry, Investig. Opthalmol. Visual Sci. 57 (2016) 126, https://doi.org/10.1167/iovs.15-18105.
[24] K. Kneipp, H. Kneipp, J. Kneipp, Surface-enhanced Raman scattering in local optical fields of silver and gold nanoaggregates - from single-molecule Raman spectroscopy to ultrasensitive probing in live cells, Acc. Chem. Res. 39 (2006) 443–450, https://doi.org/10.1021/ar050107x.
[25] S. Schumacher, L. Oeftiger, M. Mrochen, Equivalence of biomechanical changes induced by rapid and standard corneal cross-linking, using riboflavin and ultraviolet radiation, Invest. Ophthalmol. Vis. Sci. 52 (2011) 9048–9052, https://doi.org/10.1167/iovs.11-7818.
[26] J.N. Webb, J.P. Su, G. Scarcelli, Mechanical outcome of accelerated corneal crosslinking evaluated by Brillouin microscopy, J. Cataract Refract. Surg. 43 (2017) 1458–1463, https://doi.org/10.1016/j.jcrs.2017.07.037.
[27] J. Golde, F. Tetschke, J. Walther, T. Rosenauer, F. Hempel, C. Hannig, E. Koch, Detection of carious lesions utilizing depolarization imaging by polarization sensitive optical coherence tomography, J. Biomed. Opt. 23 (2018) 1, https://doi.org/10.1117/1.jbo.23.7.071203.
[28] X. Tan, A. Agrawal, D.X. Hammer, I. Ilev, Application of optical coherence tomography and optical path length method for monitoring corneal thickness and refractive index change during corneal cross-linking, Appl. Opt. 58 (2019) 4616, https://doi.org/10.1364/ao.58.004616.
[29] M.J. Ju, S. Tang, Usage of polarization-sensitive optical coherence tomography for investigation of collagen cross-linking, J. Biomed. Opt. 20 (2015), 046001, https://doi.org/10.1117/1.jbo.20.4.046001.
[30] S. Jaisson, S. Lorimier, S. Ricard-Blum, G.D. Sockalingum, C. Delevallée-Forte, G. Kegelaer, M. Manfait, R. Garnotel, P. Gillery, Impact of carbamylation on type I collagen conformational structure and its ability to activate human polymorphonuclear neutrophils, Chem. Biol. 13 (2006) 149–159, https://doi.org/10.1016/j.chembiol.2005.11.005.
[31] H.G.M. Edwards, D.W. Farwell, J.M. Holder, E.E. Lawson, Fourier-transform Raman spectroscopy of ivory: II. Spectroscopic analysis and assignments, J. Mol. Struct. 435 (1997) 49–58, https://doi.org/10.1016/S0022-2860(97)00122-1.
[32] B.G. Frushour, J.L. Koenig, Raman scattering of collagen, gelatin, and elastin, Biopolymers 14 (1975) 379–391, https://doi.org/10.1002/bip.1975.360140211.
[33] N.B. Colthup, L.H. Daly, S.E. Wiberley, Introduction to Infrared and Raman Spectroscopy, vol. 3, Acad. Press, Inc., Boston [u.a., 1990. http://slubdd.de/katalog?TN_libero_mab2730473.
[34] P. Shao, A.M. Eltony, T.G. Seiler, B. Tavakol, R. Pineda, T. Koller, T. Seiler, S.H. Yun, Spatially-resolved Brillouin spectroscopy reveals biomechanical abnormalities in mild to advanced keratoconus in vivo, Sci. Rep. 9 (2019) 1–12, https://doi.org/10.1038/s41598-019-43811-5.
[35] D. Viswanathan, N.L. Kumar, J.J. Males, S.L. Graham, Relationship of structural characteristics to biomechanical profile in normal, keratoconic, and crosslinked eyes, Cornea 34 (2015) 791–796, https://doi.org/10.1097/ICO.0000000000000434.
[36] O. Richoz, S. Kling, S. Zandi, A. Hammer, E. Spoerl, F. Hafezi, A constant-force technique to measure corneal biomechanical changes after collagen cross-linking, PLoS One 9 (2014) 3–7, https://doi.org/10.1371/journal.pone.0105095.
[37] B.J. Blackburn, M.W. Jenkins, A.M. Rollins, W.J. Dupps, A review of structural and biomechanical changes in the cornea in aging, disease, and photochemical crosslinking, Front. Bioeng. Biotechnol. 7 (2019), https://doi.org/10.3389/fbioe.2019.00066.
[38] R. Farhat, M.K. Ghannam, G. Azar, J. Nehme, M. Sahyoun, N.G. Hanna, M. Abi Karam, C. el Haber, A. Schakal, A. Jalkh, A. Samaha, Safety, efficacy, and predictive factors of conventional epithelium-off corneal crosslinking in the treatment of progressive keratoconus, J. Ophthalmol. 2020 (2020), https://doi.org/10.1155/2020/7487186.
[39] T. Koller, M. Mrochen, T. Seiler, Complication and failure rates after corneal crosslinking, J. Cataract Refract. Surg. 35 (2009) 1358–1362, https://doi.org/10.1016/j.jcrs.2009.03.035.
[40] F. Raiskup, A. Theuring, L.E. Pillunat, E. Spoerl, Corneal collagen crosslinking with riboflavin and ultraviolet-A light in progressive keratoconus: ten-year results, J. Cataract Refract. Surg. 41 (2015) 41–46, https://doi.org/10.1016/j.jcrs.2014.09.033.
[41] R. Vinciguerra, M.R. Romano, F.I. Camesasca, C. Azzolini, S. Trazza, E. Morenghi, P. Vinciguerra, Corneal cross-linking as a treatment for keratoconus: four-year morphologic and clinical outcomes with respect to patient age, Ophthalmology 120 (2013) 908–916, https://doi.org/10.1016/j.ophtha.2012.10.023.
[42] A. Caporossi, C. Mazzotta, S. Baiocchi, T. Caporossi, Long-term results of riboflavin ultraviolet A corneal collagen cross-linking for keratoconus in Italy: the siena eye cross study, Am. J. Ophthalmol. 149 (2010) 585–593, https://doi.org/10.1016/j.ajo.2009.10.021.
[43] J. Lenk, R. Herber, C. Oswald, E. Spoerl, L.E. Pillunat, F. Raiskup, Risk factors for progression of keratoconus and failure rate after corneal cross-linking, J. Refract. Surg. 37 (2021) 816–823, https://doi.org/10.3928/1081597x-20210830-01.
[44] F. Bao, Y. Zheng, C. Liu, X. Zheng, Y. Zhao, Y. Wang, L. Li, Q. Wang, S. Chen, A. Elsheikh, Changes in corneal biomechanical properties with different corneal cross-linking irradiances, J. Refract. Surg. 34 (2018) 51–58, https://doi.org/10.3928/1081597X-20171025-01.
[45] R. Herber, M. Francis, N. Nethralaya, E. Spoerl, L.E. Pillunat, Comparison of Waveform Derived Corneal Stiffness and Stress-Strain Extensometry Derived Corneal Stiffness Using Different Cross-Linking Irradiances : an Experimental Study with Air, 2020.
[46] R. Vinciguerra, V. Romano, E.M. Arbabi, M. Brunner, C.E. Willoughby, M. Batterbury, S.B. Kaye, In vivo early corneal biomechanical changes after corneal cross-linking in patients with progressive keratoconus, J. Refract. Surg. 33 (2017) 840–846, https://doi.org/10.3928/1081597X-20170922-02.